Frequency-Domain Spectroscopic Study of the PS I−CP43′ Supercomplex from the Cyanobacterium *Synechocystis* PCC 6803 Grown under Iron Stress Conditions

Kerry J. Riley,[†] Valter Zazubovich,*[,‡] and Ryszard Jankowiak*[,§]

Ames Laboratory−USDOE and Department of Chemistry, Iowa State University, Ames, Iowa 50011-3111, Department of Physics, Concordia University, 7141 Sherbrooke Street West, Montreal, Quebec H4B 1R6, Canada, and Department of Chemistry, Kansas State University, 103 Chemistry and Biochemistry Building, Manhattan, Kansas 66506-3701

Received: June 13, 2006; In Final Form: August 28, 2006

Absorption, fluorescence excitation, emission, and hole-burning (HB) spectra were measured at liquid helium temperatures for the PS I−CP43′ supercomplexes of *Synechocystis* PCC 6803 grown under iron stress conditions and for respective trimeric PS I cores. Results are compared with those of room temperature, time-domain experiments (*Biochemistry* **2003**, *42*, 3893) as well as with the low-temperature steady-state experiments on PS I−CP43′ supercomplexes of *Synechococcus* PCC 7942 (*Biochim. Biophys. Acta* **2002**, *1556*, 265). In contrast to the CP43′ of *Synechococcus* PCC 7942, CP43′ of *Synechocystis* PCC 6803 possesses two low-energy states analogous to the quasidegenerate states A and B of CP43 of photosystem II (*J. Phys. Chem. B* **2000**, *104*, 11805). Energy transfer between the CP43′ and the PS I core occurs, to a significant degree, through the state A, characterized with a broader site distribution function (SDF). It is demonstrated that the low temperature ($T = 5$ K) excitation energy transfer (EET) time between the state A of CP43′ (IsiA) and the PS I core in PS I−CP43′ supercomplexes from *Synechocystis* PCC 6803 is about 60 ps, which is significantly slower than the EET observed at room temperature. Our results are consistent with fast (≤10 ps) energy transfer from state B to state A in CP43′. Energy absorbed by the CP43′ manifold has, on average, a greater chance of being transferred to the reaction center (RC) and utilized for charge separation than energy absorbed by the PS I core antenna. This indicates that energy is likely transferred from the CP43′ to the RC along a well-defined path and that the "red antenna states" of the PS I core are localized far away from that path, most likely on the B7−A32 and B37−B38 dimers in the vicinity of the PS I trimerization domain (near PsaL subunit). We argue that the A38-A39 dimer does not contribute to the red antenna region.

Introduction

The evolution of photosynthetic organisms has resulted in the development of different strategies to adapt their photosynthetic apparatuses to various conditions of illumination or nutrient supply. One such strategy involves changing the extent and structure of phycobilisomes.[1,2] In an iron-deficient environment, the phycobiliprotein content and photosystem I (PS I) to photosystem II (PS II) ratio are reduced.[3] This is compensated by an accumulation of IsiA (CP43′)[4−6] protein, a chlorophyll *a* (Chl *a*) binding protein genetically very similar to CP43 of photosystem II (PS II).[7,8] In particular, the typical reaction of some cyanobacteria to iron stress is to surround the (trimeric) PS I core with 18[7,9,10] (or 17 for the PS I lacking PsaF and PsaJ subunits[11]) copies of CP43′. The PS I core monomer contains protein subunits PsaA to PsaX; most of the chlorophyll (Chl) molecules, including the reaction center (RC) chlorophylls, are bound to PsaA and PsaB subunits, which are approximately related to each other by C_2 symmetry.[12] An arrangement involving 18 copies of CP43′ was observed for *Synechococcus* PCC 7942[9] and *Synechocystis* PCC 6803.[10] It is interesting that a similar structural arrangement was also adopted by deep-water (low-illumination) strains of *Prochlorococcus marinus,*[13] although, in this case, antenna complexes and probably also the PS I core contain Chl b_2 (divinyl derivative of Chl *b* with similar spectral properties). Recently, several groups engaged in studying spectral properties and energy transfer dynamics in CP43′ and PS I−CP43′ supercomplexes of cyanobacteria.[14−16] These works agree that the CP43′ ring effectively transfers energy to the PS I core, although an increase of total trapping time (compared to separate PS I cores) was also observed.[14,16] Components with characteristic times from 1.7 to 10 ps observed in the *Synechocystis* CP43′ (supercomplex minus core) kinetics at room temperature have been ascribed to the CP43′ → PS I core excitation energy transfer (EET).[14] While a 1.7 ps component was assigned to the fastest EET through closely located chlorophylls at the interface between the CP43′ and the PS I core, it was suggested that the 10 ps process corresponds to the overall excitation transfer from CP43′ to the PS I core.[14] The high-resolution structure of the CP43′ complex is not known, but the three-dimensional structure of the PS I−CP43′ supercomplex has been modeled by merging low-resolution cryomicroscopy data[17] with available high-resolution data on PS I from *Thermosynechococcus elongatus*[12] and CP43 from PS II,[18] see Figure 1. Only 12 chlorophyll molecules per CP43 were identified in ref 18, and only 11 are depicted in Figure 1 and in ref 17, while according to the more recent X-ray diffraction data, there are 13 (ref 19, 20) or even 14 (ref 21)

* Corresponding authors. E-mail: vzazubov@alcor.concordia.ca (V.Z.); ryszard@ksu.edu (R.J.).
[†] Iowa State University.
[‡] Concordia University.
[§] Kansas State University.

10.1021/jp063691f CCC: $33.50
Published on Web 10/18/2006

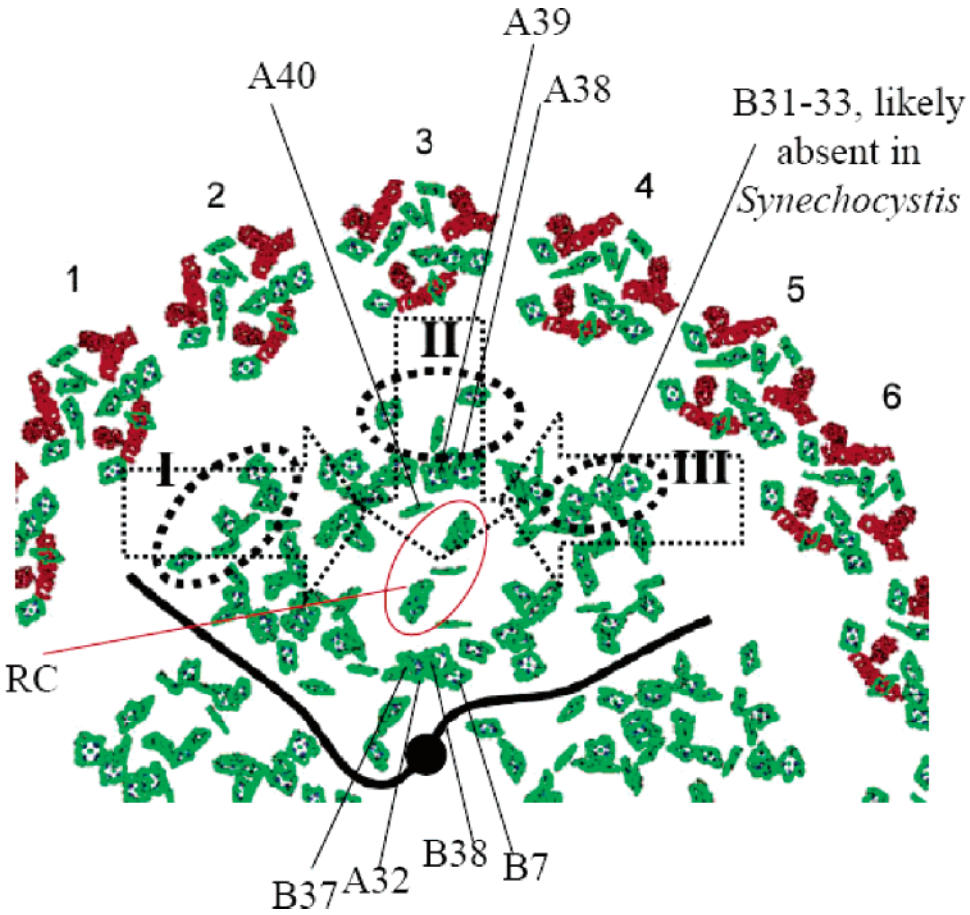

Figure 1. (Modified from ref 17.) Arrangement of trimeric PS I and CP43′ antenna complexes in the PS I−CP43′ supercomplex, based on X-ray diffraction data for PS I of *Synechococcus elongatus*[12] and CP43[18] and low-resolution cryomicroscopy data.[17] Regions of most probable CP43′ to PS I core energy transfer are labeled by Roman numbers. Arabic numbers 1−6 refer to CP43′ complexes in nonequivalent positions in relation to the PS I core monomer. Core chlorophyll molecule labeling is according to ref 12. Dotted arrows indicate most likely paths of the CP43′ to PS I core energy transfer. Dark solid circle indicates the center of the PS I trimer.

chlorophylls per CP43. However, one should be careful comparing CP43 and CP43′, because CP43′ has ∼130 fewer amino acids than CP43 due to the absence of a hydrophilic loop joining the lumenal ends of the transmembrane helices 5 and 6.[17] That said, if one assumes that the CP43′ complexes bind chlorophylls in the same way as CP43, then the closest distances between Chl *a* molecules of adjacent CP43′ complexes may be as small as 10 Å, which could result in subpicosecond energy equilibration within the CP43′ ring at room temperature. It also appears that there are three regions per PS I monomer, where Chl *a* molecules belonging to CP43′ are close enough (within ∼20 Å) to the Chl *a* molecules of the PS I core to justify excitation energy transfer on an ∼2 ps time scale at room temperature.[7,14,16,17] One of the intriguing results of ref 17 is that one of these contact regions of the PS I core incorporates chlorophylls labeled B31, B32, and B33 (labeling according to ref 12), which is a possible origin of one of the red antenna states of the PS I core[12] (see below). The second region includes chlorophylls J1−J3 and the third region, chlorophylls A8, A10, A12−A14, A18, and K2. These regions are labeled III, II, and I, respectively, in Figure 1. Note that six CP43′ complexes are in nonequivalent positions relative to the PS I core monomer (see Figure 1, see also ref 17), and therefore, the reported CP43′ → PS I core energy transfer rates may be an average of several different rates. Concerning *Synechocystis* PCC 6803, one should also remember that the B31−B33 trimer (channel III) most likely is absent or disrupted in this cyanobacterium due to the absence of histidine residues coordinating B31−B33 chlorophylls.[27]

Spectral hole burning (SHB) has been successfully applied to various photosynthetic complexes, including trimeric cyanobacterial PS I (ref 22−24) and CP43 isolated from PS II of higher plants.[25,26] The widths of spectral holes are inversely proportional to the lifetimes of the excited states. This feature makes SHB very useful in exploring energy transfer processes in photosynthetic complexes. In the case of the CP43, SHB was applied to demonstrate that this complex possesses two quasidegenerate, low-energy states, labeled A and B in ref 25, characterized by different inhomogeneous widths and different permanent dipole moment differences between the ground and excited state as well as different intersystem crossing yields. For PS I, SHB was mainly employed to resolve different red antenna states (i.e., the antenna states absorbing at lower energy than the primary donor, P700) and to prove that these states originate from aggregates of strongly coupled chlorophyll molecules (and not from monomeric Chl *a*, whose red-shifted energies are the result of peculiar interactions with the protein environment[22−24]). Three red antenna states were resolved by SHB for *Synechococcus elongatus*[22] and two for *Synechocystis* PCC 6803.[23,24] It is interesting that the lowest-energy states of the PS I of the above two cyanobacteria, C719 and C714, respectively, have very similar properties and therefore most likely originate from the same chlorophyll aggregate.[22−24]

However, there is no agreement regarding the correspondence between the red antenna states and particular chlorophyll aggregates. So far, at least 12 different Chl *a* aggregates were suggested and several combinations of them were considered.[22,27−31] The lack of agreement concerning the red-state assignments is due to the problems associated with calculating interpigment electrostatic couplings, and especially chlorophyll site energies, with sufficient precision.

Although the works[14−16] provided extensive and valuable data on the functioning of the PS I−CP43′ supercomplex, several issues remain unresolved. First, to achieve a satisfactory fit to the absorption spectra of the PS I−CP43′ supercomplex from *Synechococcus* PCC 7942, it had to be assumed that there are 17−18 Chl *a* molecules per CP43′ complex[15] rather than 13, as suggested by structural data on CP43.[18] The results of ref 15 also indicated that one of the low-energy states (i.e., B state[22]) present in CP43 could be missing in CP43′. It is unclear if those differences between CP43 and CP43′ are real or resulted from the partial disruption of the samples during the preparation/isolation procedures. Second, existing data on energy transfer for both *Synechococcus* PCC 7942 (ref 16) and *Synechocystis* PCC 6803 (ref 14) were only obtained at room temperature using ultrafast spectroscopy, which by its nature lacks spectral resolution. Therefore, the purpose of this work is to utilize high-resolution spectral hole burning (SHB) to gain additional insight into the properties of PS I−CP43′ complexes from *Synechocystis* PCC 6803 by comparing the SHB results with those previously obtained by means of time-domain spectroscopy.[14] In addition, SHB results are compared with the steady-state spectroscopy results obtained for *Synechococcus* PCC 7942.[15] Here, the goal is to determine if the lowest-energy states similar to those observed in the isolated CP43 from PS II[22] are present in CP43′ and, if so, how these states affect energy transfer from CP43′ to the PS I core.

Experimental Section

PS I trimers and PS I−CP43′ supercomplexes were isolated as described in ref 14 and stored at −77 °C. Immediately before the experiment, a sample/buffer solution was mixed with glycerol at a ratio 1:2 in order to ensure formation of good quality glass upon cooling. This mixture was placed into plastic vials 9 mm in diameter and slowly frozen in the dark in a Janis 10DT liquid helium cryostat. Temperature was measured and stabilized with a Lakeshore model 330 temperature controller.

Absorption spectra were measured with a Bruker IFS-120HR Fourier transform spectrometer with a resolution of 2 cm^{-1}. Broadband fluorescence excitation spectra were measured while scanning the laser (COHERENT CR-699 with intracavity etalons removed, i.e., with a line width of several GHz) wavelength over the whole dye range (LD688 dye, 650−720 nm) and collecting the fluorescence at $\lambda > 730$ nm with the photomultiplier (Hamamatsu), positioned at 90° angle with respect to the excitation beam. Fluorescence excitation spectra were corrected to take into account the (weak) wavelength dependence of the transmission of neutral filters. Emission spectra were measured with ∼1 nm resolution using a McPherson 2061 1-m focal length monochromator with a Princeton Instruments diode array as a detector. Samples were diluted to $OD_{680} < 0.1$ per 1 cm thickness (to avoid reabsorption) and placed into glass vials with a diameter of 1.5 mm; the vials, in turn, were placed into a Janis SVT-100 cryostat. Fluorescence was excited by an Ar-ion laser with about 15 mW at 514 nm. The collected emission spectra were corrected for the response function of the spectrometer/detector system.

Persistent hole spectra are the difference between postburn and preburn absorption spectra. Triplet bottleneck hole-burned spectra (measured after saturation of persistent holes) are the difference spectra between the absorption spectra measured with the laser on and that measured with the laser off. Nonresonant satellite hole spectra were measured with 2 cm^{-1} resolution using a Bruker IFS-120HR spectrometer. Holes used for constructing the hole-burning action spectrum (i.e., hole depth dependence on the wavelength for fixed burn dose) in absorption/transmission mode were measured with the same spectrometer at 0.5 cm^{-1} resolution. Burn intensities and times are reported in text and figure captions. Burn intensities were adjusted using neutral density filters (LOMO) and a laser power stabilizer/controller (BEOC). The COHERENT CR-699 ring dye laser with a line width of several GHz was used for hole burning. The lifetime(s) of the lowest energy state(s) of CP43′ were determined using the CR-699-29 (Autoscan) laser at 0.2 GHz resolution in fluorescence excitation mode. After a series of burns, the sample was heated in the dark to ∼150 K in order to refill the holes. After the sample cooled back to 5 K, the absorption spectrum was measured and compared to that obtained at the very beginning of the experiment to ensure that the sample was still intact and the spectral holes had been fully filled (i.e., erased).

Results

Absorption Spectra. The 5 K absorption spectra of PS I−CP43′ supercomplexes (a) and corresponding PS I cores (b) are presented in Figure 2A. The spectrum of PS I cores is almost identical to the spectra of *Synechocystis* PCC 6803 PS I reported in refs 23, 24, although the PS I explored in these works was obtained from a different source. Similar intensities of the red antenna state region in this work and refs 23, 24 indicate that the PS I cores in this work are indeed trimeric. Curve (c) in Figure 2A is the difference spectrum between absorption spectra of PS I−CP43′ and the PS I trimeric core. Before calculating the difference spectrum, the spectrum of the PS I core was renormalized so that the low-energy edges of the two spectra matched as closely as possible. (Assuming that absorption spectrum of the CP43′ ought to resemble that of the CP43 of higher plants, both should have negligible absorption at $\lambda >$ 695 nm. Thus, all absorption at $\lambda > 695$ nm should belong to the PS I core.) Therefore, the difference spectrum (curve c) should be treated as the absorption spectrum of CP43′ complexes. The main broad absorption band is located near 668.3 nm with an additional narrow peak at 681.2 nm; the intensity ratio of the two bands is ∼2:1. There is also a prominent shoulder near 675−676 nm. These spectral features are similar to those observed for CP43, where the respective bands were observed at 669, 682.4, and ∼678 nm.[25] The spectrum of CP43 from ref 25 is shown in the inset of Figure 2A (dashed line) along with the difference spectrum assigned to the CP43′ complex (solid line). It is apparent that the absorption spectra of CP43′ and CP43 are fairly similar, i.e., both contain a weak narrow band near 682 nm.

Fluorescence Excitation Spectra. The fluorescence excitation spectra of the PS I−CP43′ supercomplexes (curve d) and trimeric PS I cores (e) are presented in Figure 2B. Because a significant part of the energy harvested by the bulk antenna is transferred to the RC and not to the red-emitting states, the shapes of spectra (d) and (e) differ from the shapes of absorption spectra (a) and (b), respectively. Different shapes indicate that excitation may not fully equilibrate over the whole antenna system before being transferred to the red antenna states at low

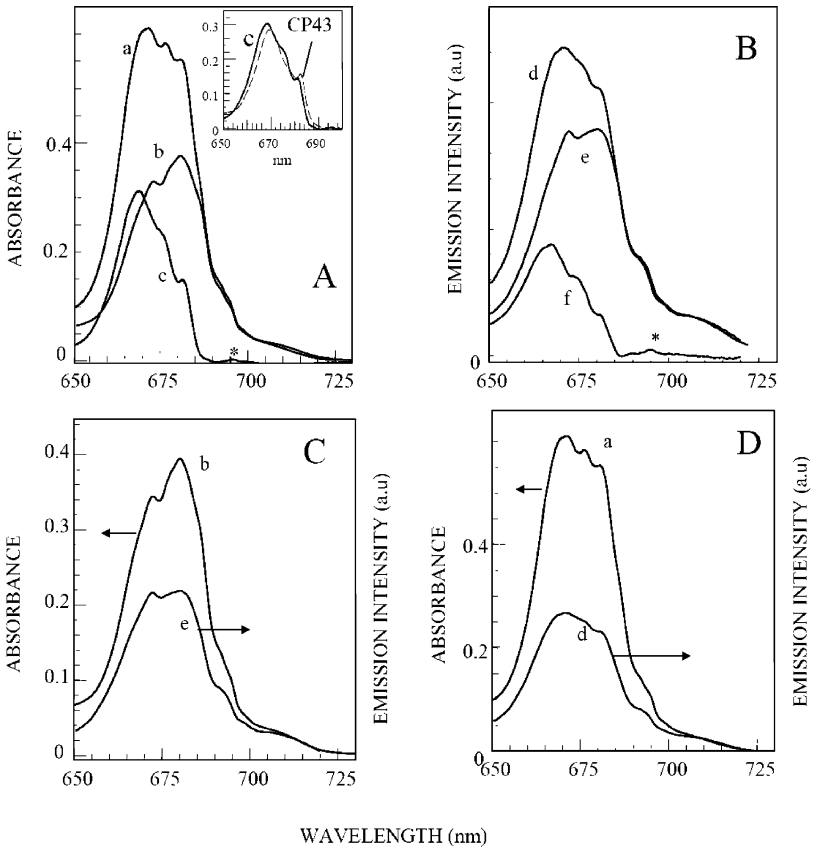

Figure 2. Frame A: 5 K absorption spectra of the PS I−CP43′ supercomplex (a), PS I core (b), and their difference spectrum ascribed to CP43′ ($c = a - b$). Insert compares 5 K absorption spectra of the CP43′ (solid curve, (c) in the main picture) and CP43 (dashed curve). Frame B: 5 K fluorescence excitation spectra of the PS I−CP43′ supercomplex (d), PS I core (e), and their difference spectrum ascribed to CP43′ (curve f). Asterisk in frames A and B refers to a weak feature at ∼695 nm, see text. Frame C: Absorption (b) and fluorescence excitation (e) spectra of the PS I core. Frame D: Absorption (a) and fluorescence excitation (d) spectra of the PS I−CP43′ supercomplex.

temperatures. In other words, the fluorescence excitation spectrum is proportional to the absorption spectrum, with the intensity of every band multiplied by the probability that the energy absorbed by the respective chlorophyll molecule will be transferred to the red antenna states. A similar effect was reported for trimeric PS I of *Synechocystis* PCC 6803 obtained from a different source[24] and for the isolated reaction center of photosystem II.[32] The difference between spectra (d) and (e) corresponds to the fluorescence excitation spectrum of the CP43′ (see curve f). As expected, spectrum (f) closely resembles the absorption spectrum of CP43′ (curve c). It contains a feature at 681 nm, although that feature is not as well resolved as that in spectrum (c). As in the case of the absorption difference (spectrum c), spectrum (f) also reveals a weak feature near 695 nm. Therefore, we suggest that this feature is not a renormalization/subtraction artifact but that it originates from the shift of the band of some core pigment(s) due to the interaction with CP43′.

Emission Spectra. Next, the nonselectively excited (at 514 nm) emission spectra of PS I−CP43′ supercomplexes and PS I cores were measured. The emission spectra of PS I−CP43′ supercomplexes obtained at various temperatures are shown in Figure 3. The spectra are qualitatively very similar to those observed for the PS I−CP43′ complex of *Synechococcus*.[15] The main fluorescence band at 720 nm with fwhm of 25 nm ($T =$ 5 K) is assigned to the emission from the C714 red antenna state of the *Synechocystis* PS I core, in agreement with ref 23. A similar but slightly narrower band (fwhm = 22 nm) red-shifted by 1 nm was observed for the PS I core sample (data not shown). The additional 685.2 nm band, observed in Figure

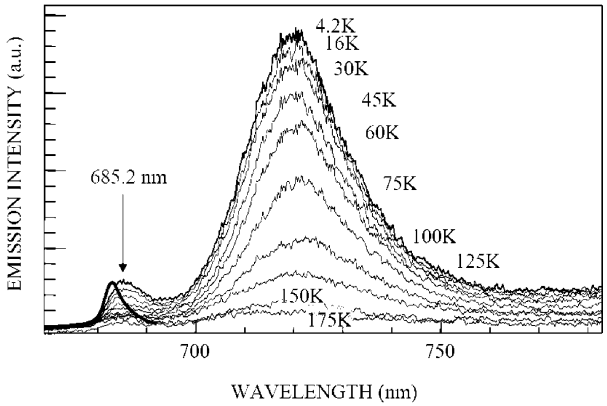

Figure 3. Thin noisy curves: emission spectra of the PS I−CP43′ supercomplex at various temperatures excited at 514 nm. Bold curve: emission spectrum of the CP43 of higher plants.[25]

3, is absent in the emission spectra of the PS I core and, therefore, most likely belongs to the CP43′. Its width is about 7 nm (150 cm^{-1}) when measured as twice the higher-energy half-width of the band. (Employing such a procedure for measuring the bandwidth is preferable because the low-energy part of the 685 nm band is contributed to by the high-energy tail of the main band peaked at 720 nm.) The ratio of the integrated areas of the 720 nm band and the 685 nm band (integrated from 670 to 800 nm) is at least 15:1 at 4.2 K. The emission spectrum of isolated CP43 from ref 25 is presented for comparison (bold curve). This spectrum is significantly

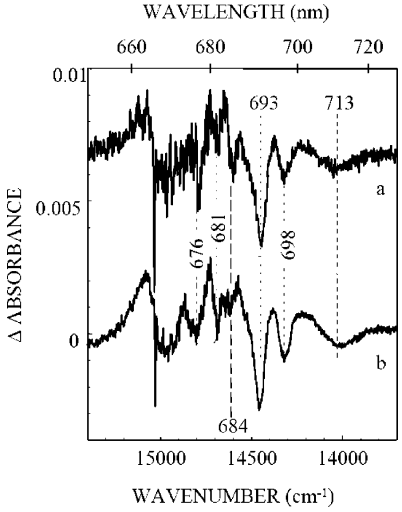

Figure 4. Spectral holes in the absorption spectra resulting at 5 K from the illumination at 665 nm with ~460 J/cm^2 for PS I−CP43′ supercomplex (a) and PS I core (b). Short-dashed lines point at the satellite hole features equally represented in both spectra. Long-dashed line refers to the hole at 684 nm, which is significantly stronger in spectrum (a).

narrower and blue-shifted by about 2 nm, compared to the emission band of the CP43′.

Hole-Burned Spectra. In the case of isolated CP43, two quasidegenerate low-energy states were reported.[25] States A and B were resolved as satellite holes using triplet bottleneck and persistent hole burning, respectively. (Satellite holes form due to hole burning following excitation energy transfer from directly excited higher-energy chlorophylls to lower-energy chlorophylls). To verify whether similar states are present in CP43′, we measured the satellite hole spectra for PS I−CP43′ and PS I core samples. Satellite persistent holes for PS I−CP43′ (a) and PS I core (b) obtained at 665 nm with laser power density of ~460 J/cm^2 are presented in Figure 4. (PS I core hole spectrum was normalized so that the PS I core absorption is equal for both samples.) For the CP43′−PS I supercomplex, the deepest satellite hole is at 693 nm, but there are also prominent holes at 676, 681, 684, and 698 nm and a broad lowest-energy hole at 713 nm. The 713 nm hole is assigned to the lowest-energy "red state" of the core, i.e., C714 state in agreement with ref 23. All of these features (except for the one at 676 nm, which is obscured by the pseudophonon sideband of a resonant hole) could be also observed at the same wavelengths upon irradiation at 670 nm (data not shown), indicating that they are not the vibronic replicas of the resonant hole. A comparison of the hole spectrum (a) to that of the PS I core (b) reveals that most of the satellite hole structure is also preserved for the PS I cores. The main difference is that the 684 nm feature is several times stronger in the PS I−CP43′ supercomplex. (Interestingly, the 681 nm persistent satellite hole obtained at similar experimental conditions was significantly deeper in the PS I core of *Synechocystis* PCC 6803 grown by a different group.[23]) No triplet bottleneck satellite holes could be observed.

Zero Phonon Hole (ZPH) Action Spectra. To gain additional insight about the number and properties of the lowest-energy states of the CP43′, we measured the hole-burning action spectra of the PS I−CP43′ supercomplexes and the PS I cores. Hole-burning action spectrum is the dependence of the hole depth on the burn wavelength for a fixed burning dose.[33] This type of spectroscopy can easily resolve the lowest-energy states of photosynthetic complexes.[25,32,33] ZPH action spectra for the

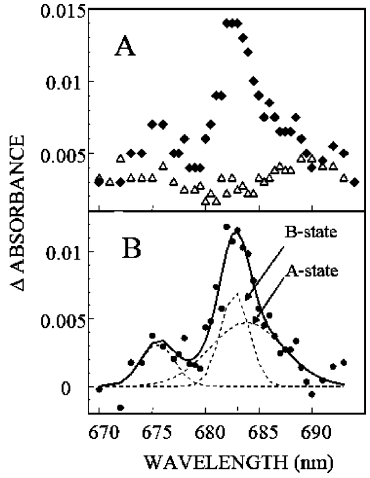

Figure 5. Frame A: 5 K hole-burning action spectra (hole depth vs wavelength for fixed burn dose) of PS I−CP43′ supercomplex (solid diamonds) and PS I core (open triangles). Burn dose was 5 J/cm^2. Frame B: Difference of the two action spectra from frame A (action spectrum of the CP43′) and its best fit.

PS I−CP43′ supercomplex and the PS I core are presented in Figure 5A. As in the case of the absorption spectra (see Figure 2), the PS I core ZPH action spectra were normalized to make the PS I core absorption equal for both samples. Only very shallow holes were observed for both the PS I−CP43′ supercomplex and PS I core at wavelengths between 695 and 705 nm (data not shown). It is interesting to note that the action spectra did not exhibit significant maxima at 693 and 698 nm, where the deepest satellite holes were observed in hole-burned spectra in Figure 4. For the results presented in Figure 5, the burn time was 1 min and the intensity 80 mW/cm^2, i.e., the burning dose was ~5 J/cm^2. Such irradiation resulted in ~3% fractional hole depths for the PS I−CP43′ supercomplex, which corresponds to ~10% holes in the CP43′ spectrum (see Figure 2A). The irradiation of PS I−CP43′ complexes with 0.5 J/cm^2 was attempted but did not yield holes with reasonable fractional depth and/or signal-to-noise ratio, at least at 0.5 cm^{-1} resolution (see below). Note that the irradiation with less than 0.5 J/cm^2 was employed with the isolated CP43[25] in order to burn ~10% deep holes. This is an indication (see Discussion for details) that the lifetime of the state(s) exhibiting persistent spectral hole burning is significantly shorter in CP43′ within the PS I−CP43′ supercomplex than that in isolated CP43. While the ZPH-action spectrum of the PS I core (triangles in Figure 5A) does not contain prominent features between 670 and 692 nm, the same cannot be said about ZPH-action spectrum obtained for the PS I−CP43′ supercomplex (diamonds). The difference of the two ZPH-action spectra (Figure 5B, circles) has two maxima at 682.5 nm and at ~676 nm. These two features must belong to the CP43′ complex. The maximum at ~682.5 nm is close to the wavelength of the nonresonantly burned hole at ~684 nm, which is strong in PS I−CP43′ and weak in PS I core (see Figure 4). While the quality of the action spectrum does not allow us to make definite conclusions concerning the number of quasidegenerate states at ~682−685 nm, a better fit to the difference of the two ZPH-action spectra (solid line in Figure 5B) involves three bands with absorption peaks/inhomogeneous widths (fwhm) of 675.6 nm/80 cm^{-1}, 682.6 nm/70 cm^{-1}, and 683.9 nm/160 cm^{-1}, respectively. The latter two bands most likely correspond to states B and A, respectively, observed in the isolated CP43.[25] The relative intensities of the two lower-energy bands in the ZPH-action spectrum are also fairly similar to those reported for isolated CP43. On the basis of its position and

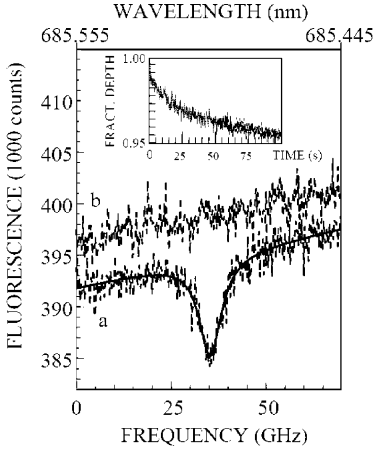

Figure 6. High-resolution hole spectrum (a) with respective preburn spectrum (b) measured in fluorescence excitation mode (noisy curves) and a Lorentzian fit (smooth thick curve) to the narrow spectral hole; fwhm = 7.3 GHz, $T = 5$ K, burning wavelength was 685.5 nm, and the burn dose was 0.1 J/cm^2. Insert: growth curve for the hole depicted in the mainframe.

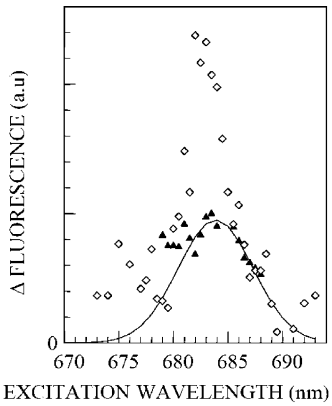

Figure 7. Hole-burning action spectra (hole depth vs wavelength for fixed burn dose) of PS I−CP43′ supercomplex obtained with 5 J/cm^2 in absorption/transmission mode (0.5 cm^{-1} resolution, open diamonds) and with 0.1 J/cm^2 in fluorescence excitation mode (0.2 GHz resolution, solid triangles). The lower-dose action spectrum is normalized to fit the solid curve, which is the broader component of the fit to the higher-dose action spectrum (see Figure 5).

width, the broader of the two lower-energy bands, which is peaked at 683.9 nm, is most likely the main origin of the 685 nm emission.

Energy Transfer Times. To determine the lifetime(s) of the lowest state(s) of the CP43′ complex (CP43′ → PS I core energy transfer times), we measured the widths of shallow holes burned into the absorption spectrum of the PS I−CP43′ supercomplex at 679−688 nm. Holes were measured in the fluorescence excitation mode. If the CP43′ complex possesses two states in this region, the contribution of the narrow band peaked at ∼682 nm to the lower-energy part (>685 nm) of this region should be negligible (see Figure 5). The shallow holes burned in this region exhibited widths of about 7−8 GHz at 5 K. The preburn absorption spectrum and the hole (burned at 685.5 nm with 0.1 J/cm^2), measured in fluorescence excitation mode along with its Lorentzian fit, are shown in Figure 6. The fractional depth of this hole is 2.5% and the width is 7.3 GHz. Assuming that about 2 GHz at 5 K is the contribution from pure dephasing,[25] one could arrive at a CP43′ → PS I core energy transfer time of about 70 ps. (Some insignificant contribution from ET between the lowest-energy states of the neighbor CP43′ complexes cannot be excluded.) It is evident from Figure 6, however, that in addition to the narrow Lorentzian hole described above, the spectra contain another, much broader component. The latter observation is in agreement with the hole-growth curve obtained for the very same hole and depicted in the inset of Figure 6, which yields fractional hole depth of ∼4% instead of 2.5%. (The hole-growth curve corresponds to the decrease in fluorescence signal, while the sample is irradiated with a laser of constant wavelength.) The similar behavior was observed for all holes burned in the 679−688 nm wavelength region, with the relative intensity of the broad contribution varying from spectrum to spectrum without apparent correlation with burn wavelength (or dose; several additional irradiation doses were employed at some wavelengths). Therefore, we did not attempt to assign that contribution or to derive any quantitative data characterizing it.

The narrow ∼7 GHz components of the holes burned with 0.1 J/cm^2 in fluorescence excitation mode were used to construct a different action spectrum, which can be compared to the one obtained in transmission/absorption mode (see Figure 5). The results are presented in Figure 7. The shape of the low-irradiation-dose ZPH-action spectrum (solid triangles) closely resembles the shape of the broader band (state A) used to fit the higher-dose, lower-resolution transmission mode action spectrum presented in Figure 5. State B does not seem to contribute significantly to the high-resolution, low-irradiation action spectrum. (This cannot be explained by sample degradation because the absorption spectrum was measured after the action spectrum depicted in Figure 7 had been obtained and that spectrum had the same shape as spectrum (a) in Figure 2A, which was acquired in the beginning of the experiment.)

Discussion

Low-Energy States of the CP43′. The main difference between the CP43′ absorption spectrum shown in Figure 2A (curve c) and that reported in ref 15 is the presence of a narrow band peaked at 681.2 nm. The inset compares curve (c) with the absorption spectrum of CP43 (ref 25) (dashed curve). Comparison reveals that spectrum (c) resembles the spectrum of CP43 much more closely than that measured for the *Synechococcus* PCC 7942 CP43′ (IsiA).[15] Our results are also consistent with the absorption spectrum reported for *Synechocystis* PCC 6803 at 77 K.[34] We hasten to add that the spectra in refs 15 and 34 were obtained directly for the isolated CP43′ complexes. Although the 681.2 nm band is somewhat weaker than the 682.5 nm band observed in CP43,[25] this characteristic band is definitely present in curve $c = a - b$ assigned (vide supra) to the CP43′ complex. Thus, by analogy with CP43, one could suggest that CP43′ possesses two quasidegenerate lowest-energy states. Further support for this assignment is provided by the hole- burning action spectra shown in Figure 5 and emission spectra in Figure 3. Because the HB data revealed that, for the lowest-energy state(s) of CP43, the electron−phonon coupling is weak,[25,26] it is unlikely that the emission peaked at 685.2 nm originates from the narrow absorption band peaked at 681.2 nm. Note that a Stokes shift of only ∼6 cm^{-1} (0.3 nm) was observed for the lowest-energy states of CP43.[25] Another important point about the emission spectra presented in Figure 3 is the relatively small intensity of the 685 nm emission in comparison with the major emission band near 720 nm. This comparison indicates that the CP43′ complexes transfer energy effectively to the PS I core.

Energy Transfer from CP43′ to the PS I Core: Analysis of the Absorption and Fluorescence Excitation Spectra. It is instructive to compare the integral intensity ratios of spectra

(a) and (b) with (d) and (e), respectively, of Figure 2. The intensity ratio of spectra (a) and (b), integrated between 600 and 730 nm, is 1.58. The integrated intensity ratio of spectra (d) and (e) is 1.33 (for 650−720 nm). The ratio difference of about 20% exceeds the error that may result from the renormalization of spectra being compared or from the difference in integration ranges. (We confirmed that the ratio of areas below (a) and (b) is still ∼1.6 for the 650−720 nm integration range. This can also be considered as an indication that the spectra in frame A are indeed superimposed properly.) Let us consider several different (d) to (e) integral intensity ratios:

The ratio of ∼1 would require that all of the energy absorbed by the CP43′ is either directly emitted from the CP43′ or transferred selectively to the RC (and consumed for charge separation) and not to the emitting red states of the core. This is because the experimental setup used to measure fluorescence excitation spectra strongly favors registration of emission at $\lambda > 730$ nm over the emission of CP43′, expected at 682−685 nm. Thus, in this case, excitation energy would not be transferred to the emitting red state of the PS I core.

A ratio of 1.58 (vide supra) would mean that all of the energy absorbed by the CP43′ is transferred to the core and then distributed between the RC and the red states in exactly the same manner as in isolated PS I core. In other words, the energy would equilibrate between the CP43′ manifold and higher-energy chlorophylls of the PS I core relatively quickly, faster than it is trapped by either RC or the red states.

A ratio larger than 1.58 (corresponding to large relative intensity of difference spectrum f) would mean that energy from the CP43′ gets preferentially transferred to the red states of the PS I core and not to the RC.

A ratio of 1.33 (i.e., between 1 and 1.58) suggests that energy absorbed by the CP43′ ring has on average a somewhat higher chance of ending up used for charge separation in the RC than the energy absorbed by the core bulk antenna states. The above arguments are valid if there is no appreciable dissipation of excitation energy within the CP43′ manifold. This assumption is supported by the similarity of the CP43′ spectra measured in absorption and fluorescence excitation modes (spectra c and f in Figure 2) and the absence of triplet bottleneck holes (vide supra). The results of the hole-burning experiments on CP43 (ref 25) also do not indicate the presence of the fast (significantly faster than fluorescence lifetime) internal conversion or intersystem crossing processes.

On the basis of results presented in ref 15 and our fluorescence data depicted in Figure 3, we assume that only a small fraction of energy absorbed by the CP43′ is emitted from the CP43′; thus for the time being, this small fraction will be ignored. We denote this fraction $P_{CP43'\_EM}$. The absorption (curve b in Figure 2A) and normalized fluorescence excitation spectrum (curve e in Figure 2B) for the PS I core are compared in frame C of Figure 2. Comparison of their integral intensities (integrated between 650 and 720 nm) reveals that about 60% of the energy absorbed by the PS I core is emitted at ∼720 nm; that is, ∼40% gets utilized for charge separation. We label this fraction as P_{core_RC}. A similar result was reported in ref 24. Following the same logic, the probability that energy absorbed by the CP43′ will be transferred to the red states of the PSI core and emitted from there, $P_{CP43'\_red\ states}$, is equal to the ratio of the (properly normalized) integrated areas of the fluorescence excitation and absorption spectra of CP43′. The latter two spectra are shown as curve (f) in Figure 2B and curve (c) in Figure 2A, respectively. Let A_{CORE} be the integral intensity (area below the spectrum) of core absorption. Then the integral intensity of the absorption spectrum of the PS I−CP43′ supercomplex will be $A_{S,Abs} = 1.58\ A_{CORE}$ and the integral intensity of the core fluorescence excitation spectrum will be $A_{C,FluorExc} = 0.6\ A_{CORE}$. The integral intensity of the supercomplex fluorescence excitation spectrum will be $A_{S,FluorExc} = 1.33 \times 0.6\ A_{CORE}$. The integral intensity of the CP43′ absorption is $A_{CP43'Abs} = A_{S,Abs} - A_{CORE} = 0.58\ A_{CORE}$ and the integral intensity of the CP43′ fluorescence excitation spectrum is $A_{CP43'FluorExc} = A_{S,FluorExc} - A_{C,FluorExc} = 0.2\ A_{CORE}$. Consequently, the $P_{CP43'\_red\ state} = 0.2\ A_{CORE}/0.58\ A_{CORE} = 34\%$, compared to 60% for the probability of transfer from the higher-energy states of the core to the red antenna states. Thus, on average, the excitation of the CP43′ indeed results in a charge separation that is significantly more efficient than that resulting from the excitation of PS I core. Thus we suggest that the energy transfer between the CP43′ ring and the reaction center of the core occurs, at least at low temperatures, along a relatively well-defined pathway, carefully avoiding the chlorophylls responsible for the "red antenna states." At the first glance, this result contradicts the widely accepted trap-limited model of energy transfer processes in the PS I core (see refs 35, 36 for review). According to that model, the energy equilibrates over the PS I core much faster than charge separation occurs; the excitation visits P700 several times before it gets photochemically trapped. However, the trap-limited model with "trap" meaning solely P700 is applicable at room temperature, when EET is possible from the lowest-energy antenna states to the P700. At lower temperatures, the photochemical trapping at P700 is accompanied by competing trapping on the lowest-energy antenna states. At 5 K, the energy can be transferred only downhill, and the very fact that charge separation can occur in about 40% of cases[37] means that, in some PS I cores (or in all cores but for a fraction of time), the excitation is transferred to the P700 without visiting the red states. It also means that the excitation either stays at P700 for a long enough time for charge separation to occur or that it migrates back and forth between P700 and some neighbor chlorophylls absorbing at the same energy as P700. This state of affairs is incompatible with complete equilibration preceding charge separation. (A similar conclusion was reached in ref 37.) Also, because at 5 K, only downhill energy transfer processes are possible, every donor can interact with much smaller number of available acceptors than at room temperature. This makes the existence of the well-defined EET pathways at this temperature all the more likely. The above argument is supported by Figure 1, which is adopted from ref 17. Dotted arrows roughly indicate the possible pathways of EET that most likely avoid the B37−B38 and A32−B7 "red aggregates".[22,27−29] It was demonstrated in refs 23, 37 that red aggregates are most likely located close to the trimerization domain of the PS I (solid black dot in Figure 1). Note that, in order to avoid being transferred to the B37−B38 and A32−B7 aggregates, the energy would likely travel to the RC through the chlorophylls labeled A38−A40. The result that the A38−A39 dimer is not responsible for a red state is in agreement with the results of ref 38 where, based on spectral shifts upon charge separation in the RC, the absorption of those chlorophylls was assigned to 680−695 nm spectral region.

We now wish to estimate the time for EET from the CP43′ to the PS I core. The excitation energy redistribution is schematically shown in Figure 8. Let E be the amount of excitation energy (EE) absorbed by the PS I−CP43′ supercomplex. Of this energy, 60% is absorbed by the PS I core and 40% by the CP43′ (based on the intensity ratio of bands b and c in Figure 2A, integrated between 650 and 720 nm). Of the

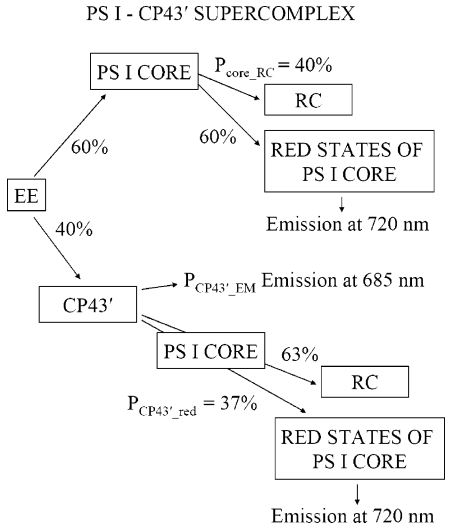

Figure 8. Scheme of the energy transfer processes between the CP43′ and the PS I core and within the PS I core.

energy absorbed by the PS I core, 60% gets emitted from the red states and 40% is utilized in charge separation. As a function of E, this amounts to 0.36 E and 0.24 E, respectively. Of the 40% of EE absorbed by the CP43′, $P_{CP43'\_EM}$ is emitted from the CP43′ and $(1 - P_{CP43'\_EM})$ is transferred to the core. As was determined above, 66% of the latter amount is utilized in charge separation and 34% is transferred to the red states and emitted from there. As a function of E, this amounts to $0.4 \times (1- P_{CP43'\_EM}) \times 0.66\ E$ and $0.4 \times (1- P_{CP43'\_EM}) \times 0.34\ E$, respectively. The total emission from the red states of the core is then $0.36\ E + 0.4 \times (1- P_{CP43'\_EM}) \times 0.34\ E = 0.496\ E - 0.136\ P_{CP43'\_EME}$. On the basis of the intensity ratio deduced from Figure 3,

$$(0.496\ E - 0.136\ P_{CP43'\_EM}\ E):(0.4\ P_{CP43'\_EM}\ E) = 15:1$$

Here we implicitly assumed that the fractions of excitations created in the CP43′ and in the PS I core upon excitation at 514 nm are the same as for excitation in the Q_y band (i.e., 40:60). This appears to be justified because the ratio of absorbance at 670 and 514 nm (that is, about 4:1) is approximately the same for CP43,[39] PS I core,[31] and PS I−CP43′ supercomplexes of *Synechococcus* PCC 7942.[15,16] Thus, we believe that the above assumption does not lead to a significant error. Solving the above equation for $P_{CP43'\_EM}$, one can arrive at a probability of ~8% for emission directly from the CP43′ at 685 nm. Taking into account this correction, we can arrive at values of 37% and 63% (instead of 34% and 66% as determined above) for the relative amounts of energy transferred from the CP43′ to the emitting red states of the PS I core and the RC, respectively; see Figure 8 for details. Thus, the conclusion that, on average, the CP43′ transfers energy to the RC much more effectively than the PS I core remains valid. Because the fluorescence lifetime of the emitting state(s) of the CP43′ is not known precisely, the knowledge of the $P_{CP43'\_EM}$ does not allow us to determine the CP43′ → PS I core energy transfer time precisely. Nevertheless, assuming a reasonably realistic fluorescence lifetime of 1 ns, the 8% probability of CP43′ emission requires energy transfer time to be (on average) close to 60 ps, in agreement with hole-burning results (see Figure 6).

To conclude this subsection, we need to discuss the possibility that we are dealing with a mixture of disconnected CP43′ and PS I cores. If this is true, the above argument is invalid. On the basis of data shown in Figure 2A, approximately 40% of all excitation energy would be absorbed by CP43′s and about 60% by the PS I cores. Recall that the fluorescence yield of the PS I cores at liquid helium temperatures is about 60% for excitation at wavelengths shorter than 700 nm (this percentage was determined by comparing spectra (b) and (e) in frames 2A and B after normalizing them to equal oscillator strength of the red antenna state region (Figure 2C); see also Figure 4 in ref 24). Thus, the 720 and 685 nm band integral intensity (area) ratio should be about 1:1 if no EET from CP43′ to PS I took place. Because the observed ratio is at least 15:1, this scenario can be excluded. (We assumed, again, that there is not much nonradiative energy dissipation within the CP43 or CP43′ complexes, consistent with the similarity of spectra (c) and (f) in frames A and B respectively of Figure 2 and the absence of triplet bottleneck holes.) One may also suggest that a small fraction of the CP43′ complexes (or CP43′ aggregates[34]) are disconnected from the PS I cores, and only these disconnected CP43′ complexes are the origin of the 685 nm emission. This suggestion, however, contradicts the observation that the temperature dependence of the intensity of the 685 nm emission band (not shown) is much faster than for the isolated CP43′ of *Synechococcus*.[15] Namely, by 120 K the intensity of the 685 nm band falls to about 25% of its 5 K value for supercomplexes (a similar result was reported for supercomplexes from *Synechococcus* PCC 7942 (ref 15)) and to 65% of its 5 K value for isolated CP43′ (IsiA).[15]

Energy Transfer from CP43′ to the Core: Spectral Hole Burning. The presence of a noticeable persistent satellite hole near 684 nm shown in Figure 4 is in good agreement with a noticeable 685 nm emission. Absence of triplet bottleneck holes upon nonresonant higher-energy excitation in the case of the CP43′ within the supercomplexes indicates that either the lifetime, or the intersystem crossing yield, or triplet lifetime of state A, are significantly reduced in CP43′ of the PS I−CP43′ supercomplex, compared to the isolated CP43. Overall, there are several competing decay processes with different rates for the A state of the CP43′ complex within the PS I−CP43′ supercomplex: τ_{EET}^{-1}, τ_{ICS}^{-1}, and τ_{fluor}^{-1}, which are the rate of the EET to the PS I core, the intersystem crossing rate, and fluorescence rate, respectively. (Even for the best hole-burning systems the hole-burning rate $\tau_{HB}^{-1} < 0.1 - 0.01\ \tau_{fluor}^{-1}$ (ref 40)). Of the processes mentioned above, only energy transfer to the core is absent in case of the isolated CP43. Assuming that the properties of state A in CP43 and CP43′ are otherwise similar, it is most likely that excitation energy transfer to the core competes with the intersystem crossing in the PS I−CP43′ complex. In CP43′, the energy transfer to the PS I core takes place in about 60−70 ps (vide supra); such fast EET could indeed suppress the triplet bottleneck hole formation if intersystem crossing rates are in the ns^{-1} range, typical for Chl *a*.[41] Consequently, energy transfer from the CP43′ to the PS I core occurs, to a significant degree, through state A.

Hole-burning results of Figure 6 indicate the 60−70 ps energy transfer from state A but suggest that there might be more than one energy transfer rate from the CP43′ to the PS I core. Note that six CP43′ complexes are in nonequivalent positions in relation to the PS I core monomer (see Figure 1) and, therefore, multiple rates of energy transfer from the CP43′ to the PS I core should be expected. Results presented in Figure 7 indicate that there is no significant contribution from the state B to the low-fluence fluorescence excitation mode ZPH-action spectrum, which is an indication of the short lifetime of the B state. This is in agreement with the absence of the B-state emission in Figure 3. The CP43′ emission band would be narrower and less

red-shifted than that observed if a significant amount of emission from the B state were present. (See the emission spectrum of CP43 from ref 25 superimposed in Figure 3. A significant fraction of CP43 emission originates from the narrower B state.) Another possibility to be considered is that energy from state B of the CP43′ is transferred exclusively to the reaction center of the PS I and not to the red-emitting states of the core. This would make state B unobservable in the fluorescence excitation mode regardless of its lifetime. Taking into account the architecture of the PS I−CP43′ supercomplex and the fact that some RCs are permanently closed,[42] this possibility is highly unlikely. Consequently, one must conclude that the (average) lifetime of state B is significantly shorter than that of state A. Unfortunately, precise determination of the excited-state lifetime of the state B by means of spectral hole burning is difficult because one cannot access this state selectively. However, the widths of spectral holes used to compose the action spectrum in Figure 5 can be used for rough estimation. The widths of the shallow holes burned in the absorption spectrum at ∼682 nm were in the range of 1.2−1.5 cm^{-1}, which corresponds to the lifetime of about 10 ps. Because the holes burned at ∼682 nm contain contributions from both A and B states and because the A-state contribution most likely has the resolution-limited width (0.5 cm^{-1}), 10 ps should be considered an upper limit for the B-state lifetime.

To summarize, we are left with a relatively fast (<10 ps) energy transfer *from* state B. The nature of the acceptor in this energy transfer process (PS I core versus the state A of the CP43′) is to be determined. In this respect, three scenarios are possible, each leading to certain contradictions either with some results of this work or with the interpretations of the results obtained in ref 25 for isolated plant CP43. Before we describe these three scenarios, it is necessary to remind the reader that the structural origin of the lowest-energy band(s) of the CP43 is still unknown. It was suggested in ref 25 that both states A and B are localized on monomeric chlorophylls. In ref 43, it was argued that chlorophylls labeled 10, 18, and especially 12, are most likely to transfer energy to the PS II RC. In ref 44, the lowest-energy state of CP43 was assigned to the lowest excitonic state of the aggregate containing chlorophylls 9, 13, and 19 in the notation of ref 43. (Different notation was used in ref 44, which may be obtained by adding 14 to the notation of ref 43.) In ref 21, the lowest state of CP43 was assigned to the aggregate consisting of chlorophylls 11, 13, and 16.

In the first scenario, which is in agreement with ref 25, the state B serves as a fast (several ps) main channel for energy transfer from the CP43′ to the PS I core. However, taking into account that the energy transfer from the state A to the PS I core occurs in 60−70 ps, it is difficult to explain the relatively high intensity of the 685 nm emission band for the PS I−CP43′ supercomplex (Figure 3).

In the second scenario, we invoke fast and effective energy transfer from state B to state A in CP43′ (with state A being the main trap and the main channel for energy transfer to the PS I core). This scenario successfully explains the observations in this work, but contradicts the arguments from ref 25, where it was suggested that the B state is the primary low-energy trap of the isolated CP43, that energy transfer between the CP43 and the reaction center of the PS II occurs predominantly through state B, and that the energy transfer between states A and B is possible but very slow (∼ns).

According to the third scenario, states A and B both originate from the same chlorophyll molecule or group of molecules. The CP43′ (isolated or in the PS I−CP43′ supercomplex) samples and isolated CP43 samples explored in refs 25, 26, 39 must have been highly heterogeneous, with some CP43 or CP43′ complexes having their lowest-energy chlorophyll(s) in a very well-defined protein pocket (B-type), and the rest of the complexes having a much worse defined protein pocket (A-type). Differences in spectra between CP43 and CP43′ from different sources could then be explained by different preparations of CP43 and CP43′ containing different proportions of A-type and B-type complexes. Although B-type CP43′ complexes would transfer energy to the PS I core faster than the A-type CP43′ complexes, due to a relatively small percentage of the B-type complexes, the average transfer rate would not be significantly affected. The transition from B-type to A-type results in a nearly 2-fold increase of the permanent dipole moment change $\Delta\mu$,[25] the change of the mean phonon frequency from 24 to 15 cm^{-1},[26] and at least in case of the CP43′, a ∼7−10-fold decrease of the rate of EET to the PS I core, vide supra. However, large variations in the properties of the same chlorophyll(s) as described above were never observed for any other photosynthetic complex. In the case of the reaction center of PS II, the isolation process resulted in the shift of the P680 band from ∼684 to ∼680 nm in a majority of RCs,[32,45] but other properties of the band remained practically unchanged.[32] Moreover, the PS I−CP43′ supercomplexes were not subjected to the biochemical procedures employed for isolating CP43, and the chlorophylls serving as the energy transfer channel from the CP43′ to the PS I core are not as exposed to the environment as those in isolated CP43. Therefore, the most apparent reasons for disruptions leading to several different types of the same lowest state in CP43 are absent in case of CP43′ in the intact supercomplexes, and the scenario involving heterogeneity of CP43 and CP43′ samples is quite unlikely. On the other hand, there is not enough evidence available at the moment to completely reject that scenario.

Presuming that the results obtained for CP43′ in this work must have larger "weight" than those obtained for a different system (isolated plant CP43), we favor the second scenario, involving fast B → A energy transfer. More research, especially on the isolated CP43 and CP43′, is needed to clarify if the results obtained for the CP43 need reinterpretation.

Quality of the Samples and Pigment Content of the CP43′ Complexes. To determine the pigment content of the CP43′ complexes, the areas under the PS I−CP43′ and the PS I core absorption spectra and their difference (assigned to CP43′) in Figure 2A were determined in the wavelength range from 600 to 730 nm. These areas (which include Q_y origin and its vibronic replicas) scale approximately as 5.2:3.3:1.9. Assuming that there are 96 Chl *a* molecules per PS I core monomer[12] and that the PS I−CP43′ supercomplex contains 18 CP43′ complexes, one can conclude that the number of Chl *a* molecules in CP43′ is about 10, which is closer to the 13 that were found in CP43 by means of X-ray diffraction[19,20] than the 17−18 molecules reported in ref 15. The discrepancy between 10 and 13 may be explained if one remembers that, due to electrostatic interactions between chlorophyll molecules in the adjacent CP43′ complexes as well as in the CP43′ and the PS I core, the spectrum of PS I−CP43′ may differ from the sum of the spectra of the PS I core and 18 CP43′s even if the complexes are not disrupted. This possibility was not considered when renormalizing the PS I core absorption spectrum to the lower-energy edge of the PS I−CP43′ absorption spectrum. Electrostatic interactions between chlorophyll molecules of PS I core and CP43′ may also be a reason for the weak (less than 0.2 Chl *a* equivalent) features marked by an asterisk in spectra (c) and (f) in Figures 2A and

B, respectively. However, it is also possible that our PS I−CP43′ supercomplexes could miss some of the 18 CP43′ subunits, and/or that the intact CP43′ might indeed contain only 10 Chl *a* molecules per complex. The former possibility is more likely, as it agrees with the results of ref 34. In that work, 77 K absorption and fluorescence excitation spectra of PS I−CP43′ complexes from *Synechocystis* PCC 6803 with different CP43′ content were presented. While the spectra of the PS I−CP43′ with exactly 18 CP43′ complexes per PS I trimer were somewhat less structured than the spectra presented in this work, the spectra of the complexes with less than 18 CP43′ per PS I trimer more closely resembled our 5 K spectra. On the basis of the results of ref 34, the results of ref 15, in which the CP43′ chlorophyll content was estimated as 17−18, could be explained assuming that the CP43′ content was higher than 18 per PS I trimer in that work. The formation of a second CP43′ ring around the first ring of the CP43′ complexes was observed for supercomplexes from *Synechocystis* grown under prolonged iron stress conditions.[34] In this respect, it is interesting to note that the 5 K absorption spectrum of the CP43′ complex from *Synechococcus* published in ref 15 lacks the structure present in the spectrum (c) in Figure 2A and in the spectra of ref 34, even though the latter were collected at 77 K and consequently should be less structured than the 5 K spectra. Although we do not want to engage in speculations about the origin of the spectra belonging to the different bacterium, we find it worthwhile to mention that less-structured CP43′ spectra were obtained in our laboratory after the sample was accidentally heated while under illumination by the FT spectrometer white light beam. (Moderate heating of the sample in the dark, to about 150 K, typically used to refill the spectral holes, vide supra, returned the shape of the absorption spectrum to that observed in the beginning of experiment.) The spectra in this work can be best fitted by assuming that there are 13 Chl *a* molecules per CP43′ if there are ∼15 CP43′ units per PS I core *trimer*. Aggregates with 12−14 CP43′ units surrounding the PS I core *monomer* were observed in ref 34. However, the spectra expected from the latter system would be quite different from those presented in Figure 2. We conclude that the presence of supercomplexes where the PS I core monomer is surrounded by the CP43′ units is quite unlikely in samples studied in this work.

Conclusions

We have demonstrated that low-temperature energy transfer between the CP43′ manifold and the PS I core is very effective in PS I−CP43′ supercomplexes from *Synechocystis* PCC6803. Average transfer time is about 60 ps. This finding is consistent with very efficient energy transfer ($\tau_{EET} \leq 10$ ps) observed for the same system at room temperature. The CP43′ of *Synechocystis* PCC 6803 possesses two low-energy states analogous to the quasidegenerate states A and B of CP43 of photosystem II. Energy transfer between the CP43′ and the PS I core occurs to a significant degree through the broader state A. (Possible implications of these results for CP43, including the possibility of fast energy transfer between states A and B, will be the subject of future publication.) It was also demonstrated that energy absorbed by the CP43′ manifold has, on average, a higher chance to be transferred to the RC and utilized for charge separation than energy absorbed by the PS I core. Thus, at low temperatures, the energy transfer from CP43′ to the RC occurs along a relatively well-defined path, avoiding the chlorophylls responsible for the "red antenna states." This indicates that the "red antenna states" of the PS I core are most likely localized on the aggregates B7−A32 and B37−B38 located close to the PS I trimerization domain (near PsaL subunit). We also argue that the A38−A39 aggregate unlikely contributes to the red antenna region. The lower limit of the chlorophyll content of CP43′ was estimated to be close to 10. However, we consider it more likely that the chlorophyll content of the CP43′ is closer to 13 (observed for CP43), but the number of CP43′ complexes per PS I trimer in our samples was smaller than 18 (i.e., it is most likely ∼15). In addition, the content of CP43′ monomers or CP43′ aggregates disconnected from the PS I cores in our samples was negligible. The similarity of results obtained for *Synechocystis* PCC 6803 in this work and *Synechococcus* PCC 7942[15] may indicate that either B31−B33 trimer is absent/disrupted also in the latter cyanobacterium or that it does not act as a main energy transfer channel between CP43′ and the PS I core. It would be very interesting to perform experiments analogous to those described in this work on the PS I−CP43′ supercomplexes from *Termosynechococcus elongatus*, if and when such samples become available.

Acknowledgment. This research was supported by the Division of Chemical Sciences, Office of Basic Energy Sciences, USDOE. Ames Laboratory is operated for USDOE by Iowa State University under contract W-7405-Eng-82. We are thankful to Drs. Alexander Melkozernov and Robert Blankenship (ASU) for their valuable comments, to Drs. Tõnu Reinot (ISU) and Nhan Dang (KSU) for help with fluorescence excitation spectra measurements, and to Dr. James Barber (Imperial College, London), who provided the CP43′−PS I supercomplex samples.

References and Notes

(1) Gantt, E. *BioScience* **1975**, *25*, 781.
(2) Glazer, A. N. *Annu. Rev. Microbiol.* **1982**, *36*, 173.
(3) Pakrasi, H. B.; Riethman, H. C.; Sherman, L. A. *Proc. Natl. Acad. Sci. U.S.A.* **1985**, *82*, 6903.
(4) Guikema, J.; Sherman, L. A. *Plant Physiol.* **1983**, *73*, 250.
(5) Laudenbach, D.; Strauss, N. A. *J. Bacteriol.* **1988**, *170*, 5018.
(6) Burnap, R. L.; Troyan, T.; Sherman, L. A. *Plant Physiol.* **1993**, *103*, 893.
(7) Bibby, T. S.; Nield, J.; Barber, J. *J. Biol. Chem.* **2001**, *276*, 43246.
(8) Bricker, T. M.; Frankel, L. K. *Photosynth. Res.* **2002**, *72*, 131.
(9) Boekma, E. J.; Hifney, A.; Yakushevska A. E.; Piotrowsky, M.; Keegstra W.; Berry, S.; Michel, K.-P.; Pistorius, E. K.; Kruip, J. *Nature* **2001**, *412*, 745.
(10) Bibby, T. S.; Nield, J.; Barber, J. *Nature* **2001**, *412*, 743.
(11) Kouril, R.; Yeremenko, N.; D'Haene, S.; Yakushevska, A. E.; Keegstra, W.; Matthijs, H. C. P.; Dekker, J. P.; Boekema E. J. *Biochim. Biophys. Acta* **2003**, *1607*, 1.
(12) Jordan, P.; Fromme, P.; Witt, H. T.; Klukas, O.; Saenger, W.; Krauss, N. *Nature* **2001**, *411*, 909.
(13) Bibby, T. S.; Nield, J.; Partensky, F.; Barber, J. *Nature* **2001**, *413*, 590.
(14) Melkozernov, A. N.; Bibby, T. S.; Lin, S.; Barber, J.; Blankenship, R. E. *Biochemistry* **2003**, 42, 3893.
(15) Andrizhiyevskaya, E. G.; Schwabe, T. M. E.; Germano, M.; D'Haene, S.; Kruip, J.; van Grondelle, R.; Dekker, J. P. *Biochim. Biophys. Acta* **2002**, *1556*, 265.
(16) Andrizhiyevskaya, E. G.; Frolov, D.; van Grondelle, R.; Dekker, J. P. *Biochim. Biophys. Acta* **2004**, *1656*, 104.
(17) Nield, J.; Morris, E. P.; Bibby, T. S.; Barber, J. *Biochemistry* **2003**, *42*, 3180.
(18) Zouni, A.; Witt, H.-T.; Kern, J.; Fromme, P.; Krauss, N.; Saegner, W.; Orth, P. *Nature* **2001**, *409*, 739.
(19) Kamiya, N.; Shen, J.-R. *Proc. Natl. Acad. Sci. U.S.A.* **2003**, *100*, 98.
(20) Biesiadka, J.; Loll, B.; Kern, J.; Irrgang, K.-D.; Zouni, A. *Phys. Chem. Chem. Phys.* **2004**, *6*, 4733.
(21) Ferreira, K. N.; Iverson, T. M.; Maghlaoui, K.; Barber, J.; Iwata, S. *Science* **2004**, *303*, 1831.
(22) Zazubovich, V.; Matsuzaki, S.; Johnson, T. W.; Hayes, J. M.; Chitnis, P. R.; Small, G. J. *Chem. Phys.* **2002**, *275*, 47.
(23) Rätsep, M.; Johnson, T. W.; Chitnis, P. R.; Small, G. J. *J. Phys. Chem. B* **2000**, *104*, 836.

(24) Hsin, T.-M.; Zazubovich, V.; Hayes, J. M.; Small, G. J. *J. Phys. Chem. B* **2004**, *108*, 10515.

(25) Jankowiak, R.; Zazubovich, V.; Rätsep, M.; Matsuzaki, S.; Alfonso, M.; Picorel, R.; Seibert, M.; Small, G. J. *J. Phys. Chem. B* **2000**, *104*, 11805.

(26) Hughes, J. L.; Prince, B. J.; Peterson Årsköld, S.; Krausz, E.; Pace, R. J.; Picorel, R.; Seibert, M. *J. Lumin.* **2004**, *108*, 131.

(27) Sener, M. K.; Lu, D.; Ritz, T.; Park, S.; Fromme, P.; Schulten, K. *J. Phys. Chem. B* **2002**, *106*, 7948.

(28) Damjanovic, A.; Vaswani, H. M.; Fromme, P.; Fleming, G. R. *J. Phys. Chem. B* **2002**, *106*, 10251.

(29) Byrdin, M.; Jordan, P.; Krauss, N.; Fromme, P.; Stehlik, D.; Schlodder, E. *Biophys. J.* **2002**, *83*, 433.

(30) Balaban, T. S. *FEBS Lett.* **2003**, *545*, 97; erratum *FEBS Lett.* **2003**, *547*, 235.

(31) Gobets, B.; van Stokkum, I. H. M.; van Mourik, F.; Dekker, J. P.; van Grondelle, R. *Biophys. J.* **2003**, *85*, 3883.

(32) Riley, K.; Jankowiak, R.; Rätsep, M.; Small, G. J.; Zazubovich, V. *J. Phys. Chem. B* **2004**, *108*, 10346.

(33) Reddy, N. R. S.; Picorel, R.; Small, G. J. *J. Phys. Chem.* **1992**, *96*, 6458.

(34) Yeremenko, N.; Kouril, R.; Ihalainen, J. A.; D'Haene, S.; van Oosterwijk, N.; Andrizhiyevskaya, E. G.; Keegstra, W.; Dekker, H. L.; Hagemann, M.; Boekma, E. J.; Matthijs, H. C. P.; Dekker, J. P. *Biochemistry* **2004**, *43*, 10308.

(35) Melkozernov, A. N. *Photosynth. Res.* **2001**, *70*, 129.

(36) Melkozernov, A. N.; Barber, J.; Blankenship, R. E. *Biochemistry* **2006**, *45*, 331.

(37) Pålsson L.-O.; Fleming, C.; Gobets, B.; van Grondelle, R.; Dekker, J.; Schlodder, E. *Biophys. J.* **1998**, *74*, 2611.

(38) Dashdorj, N.; Xu, W.; Martinsson, P.; Chitnis, P. R.; Savikhin, S. *Biophys. J.* **2004**, *86*, 3121.

(39) Groot, M.-L.; Frese, R. N.; de Weerd, F. L.; Bromek, K.; Pettersson, Å.; Peterman, E. J. G.; van Stokkum, I. H. M.; van Grondelle, R.; Dekker, J. P. *Biophys. J.* **1999**, *77*, 3328.

(40) Reinot, T.; Zazubovich, V.; Hayes, J. M.; Small, G. J. *J. Phys. Chem. B* **2001**, *105*, 5083.

(41) Correa, D. S.; de Boni, L.; dos Santos, D. S., Jr.; Barbosa Neto, N. M.; Oliveira, O. N., Jr.; Misoguti, L.; Zilio, S. C.; Mendonca, C. R. *Appl. Phys. B* **2002**, *74*, 559.

(42) Brettel, K. *Biochim. Biophys. Acta* **1997**, *1318*, 322.

(43) Vasil'ev, S.; Orth, P.; Zouni, A.; Owens, T. G.; Bruce, D. *Proc. Natl. Acad. Sci. U.S.A.* **2001**, *98*, 8602.

(44) de Weerd, F. L.; van Stokkum, I. H. M.; van Amerongen, H.; Dekker, J. P.; van Grondelle, R. *Biophys. J.* **2002**, *82*, 1586.

(45) Peterson Årsköld, S.; Prince, B. J.; Krausz, E.; Smith, P. J.; Pace, R. J.; Picorel, R.; Seibert, M. *J. Lumin.* **2004**, *108*, 97.